Phoxite, $(NH_4)_2Mg_2(C_2O_4)(PO_3OH)_2(H_2O)_4$, the first phosphate-oxalate mineral

Anthony R. Kampf[1],*, Aaron J. Celestian[1], Barbara P. Nash[2], and Joe Marty[3]

[1]Mineral Sciences Department, Natural History Museum of Los Angeles County, 900 Exposition Boulevard, Los Angeles, California 90007, U.S.A.
[2]Department of Geology and Geophysics, University of Utah, Salt Lake City, Utah 84112, U.S.A.
[3]5199 East Silver Oak Road, Salt Lake City, Utah 84108, U.S.A.

Abstract

Phoxite, $(NH_4)_2Mg_2(C_2O_4)(PO_3OH)_2(H_2O)_4$, is a new mineral species from the Rowley mine, Maricopa County, Arizona, U.S.A., and it has potential uses in agricultural applications for soil conditioning, fertilizing, and as a natural pesticide. It was found in an unusual bat-guano-related, post-mining assemblage of phases that include a variety of vanadates, phosphates, oxalates, and chlorides, some containing NH_4^+. Other secondary minerals found in association with phoxite are antipinite, aphthitalite, bassanite, struvite, thenardite, and weddellite. Crystals of phoxite are colorless composite blades up to about 0.4 mm. The streak is white, and the luster is vitreous to oily. The Mohs hardness is 2½, the tenacity is brittle, fracture is irregular, there is fair {100} cleavage, and the measured density is 1.98(2) g/cm³. Phoxite is optically biaxial (–) with $\alpha = 1.499(1)$, $\beta = 1.541(1)$, $\gamma = 1.542(1)$ (white light); $2V = 16(1)°$; dispersion $r < v$, slight; orientation $Y = \mathbf{b}$, $X \wedge \mathbf{a} \approx 9°$ in obtuse β. Electron microprobe analyses yielded the empirical formula $[(NH_4)_{1.77}K_{0.23}]_{\Sigma2}Mg_{2.00}(C_2O_4)(PO_3OH)_2(H_2O)_4$, with the C and H content inferred from the crystal structure. Raman spectroscopy confirmed the presence of NH_4 and C_2O_4. Phoxite is monoclinic, $P2_1/c$, with $a = 7.2962(3)$, $b = 13.5993(4)$, $c = 7.8334(6)$ Å, $\beta = 108.271(8)°$, $V = 738.07(7)$ Å³, and $Z = 2$. In the crystal structure of phoxite ($R_1 = 0.0275$ for 1147 $I_o > 2\sigma I$ reflections), bidentate linkages between C_2O_4 groups and Mg-centered octahedra yield chains, which link to one another via PO_3OH tetrahedra to create undulating $[Mg_2(C_2O_4)(PO_3OH)_2(H_2O)_4]^{2-}$ sheets. Strong hydrogen bonds link the sheets into a "soft framework," with channels containing NH_4^+. The NH_4^+ forms both ordered hydrogen bonds and electrostatic bonds with O atoms in the framework. Phoxite is the first mineral known to contain both phosphate and oxalate groups as essential components.

Keywords: Phoxite, new mineral species, phosphate, oxalate, crystal structure, Rowley mine, Arizona

Introduction

In our investigations of post-mining mineralization in mines of the southwestern U.S., we encountered an unusual and still actively forming bat guano assemblage at depth (125 feet) in the Rowley mine near Theba, Arizona. Previously, from this assemblage, we reported on the new mineral rowleyite, which has a microporous vanadate-phosphate framework structure (Kampf et al. 2017). Herein, we report on the new mineral phoxite, $(NH_4)_2Mg_2(C_2O_4)(PO_3OH)_2(H_2O)_4$, which is the first mineral found to contain both phosphate and oxalate groups.

Oxalate minerals are relatively rare. While they sometimes form abiotically, they most commonly occur in connection with biological systems. Some plants (e.g., *Tragia ramosa*) use calcium oxalate as a natural defense against pests and in other biochemical processes (e.g., metal detoxification and calcium regulation; Nakata 2003). Engineered calcium oxalate crystals are being studied as a novel pesticide for chewing pests (e.g., locusts) (Nakata 2015). Oxalate materials could even be employed simultaneously as pesticides and fertilizers, enriching the soil with ammonium (similar to zeolite uses; Bernardi et al.

2016; Eroglu et al. 2017) and phosphate, while providing essential oxalate ingredients to enhance natural defense mechanisms in plants. Recent developments in metal organic framework synthesis have predominantly used Fe^{2+}-based amine-templated oxalate phosphates with some success (cf. Reháková et al. 2004; Anstoetz et al. 2015; Usman et al. 2018). However, iron release can decrease soil pH and, therefore, be problematic in areas with already acidic soils. A synthetic phase corresponding to phoxite might be useful in agriculture applications with either high or low acidic soils or in soils with saline or alkaline waters. We are currently investigating methods of synthesis, ion-exchange mechanisms for common metal nutrients, and dissolution properties in phoxite, with an eye toward natural soil remediation and enhanced time-release fertilization for increased crop yield with minimal soil treatment.

Biologically induced mineralization can involve various processes among which is the deposition of excretion from birds or bats on rock surfaces to form incrustations of guano. Bat guano is generally rich in ammonium oxalate (and urate) and phosphates, as well as cations such as K, Na, Ca, Mg, and Fe. Clearly, the new mineral is compositionally consistent with formation in a guano deposit; however, it is surprising that no other mineral containing both essential phosphate and oxalate has previously

* E-mail: akampf@nhm.org

been reported from a guano deposit.

The name "phoxite" reflects the fact that the mineral contains both phosphate (ph) and oxalate (ox) groups. The new mineral and name were approved by the Commission on New Minerals, Nomenclature and Classification of the International Mineralogical Association (IMA 2018-009). Four small co-type specimens are deposited in the collections of the Natural History Museum of Los Angeles County, Los Angeles, California, U.S.A., catalog numbers 66697, 66698, 66699, and 66700.

OCCURRENCE

Phoxite was found by two of the authors (A.R.K. and J.M.) on the 125-foot level of the Rowley mine, near Theba, Painted Rock district, Maricopa County, Arizona, U.S.A. (33°2′57″N 113°1′49.59″W). The Rowley mine is a former Cu-Pb-Au-Ag-Mo-V-baryte-fluorspar mine that exploited veins presumed to be related to the intrusion of an andesite porphyry dike into Tertiary volcanic rocks. Although the mine has not been operated for ore since 1923, collectors took notice of the mine as a source of fine wulfenite crystals around 1945. The most detailed recent account of the history, geology, and mineralogy of the mine was given by Wilson and Miller (1974).

The new mineral was found in a hot and humid area of the mine in an unusual bat-guano-related, post-mining assemblage of phases that include various vanadates, phosphates, oxalates, and chlorides, some containing NH_4^+. This secondary mineral assemblage is found growing on baryte-quartz-rich matrix. Phoxite was found near the floor of the tunnel in close association with antipinite (second known occurrence; Chukanov et al. 2015), aphthitalite, bassanite, struvite, thenardite, and weddellite, as well as bat-related biological residue. Phoxite crystal intergrowths comprise portions of the interiors and rims of circular masses, presumably related to relatively recent/fresh bat excrement (Fig. 1). Other secondary minerals found in this general assemblage include ammineite, cerussite, fluorite, halite, hydroglauberite, mimetite, mottramite, perite, rowleyite (Kampf et al. 2017), salammoniac, urea, vanadinite, willemite, wulfenite, and several other potentially new minerals.

Phoxite has also been verified to occur in Petrogale Cave, near Madura, Western Australia (31°52′9″S 127°23′19″E). Bridge (1977) reported it as a phase associated with archerite and designated it as *unknown A*. It is listed as UM1977-10-PO:CaClKMg on the IMA list of Valid Unnamed Minerals. As the latter designation indicates, it was determined by Bridge to contain P, K, Ca, Mg, and minor Cl. The equivalence of Bridge's *unknown A* to phoxite was reported to the authors by Peter Elliott, who has restudied the original samples of Bridge (1977). The K, Ca, and Cl in Bridge's preliminary electron probe microanalysis are apparently nonessential components, and Bridge presumably did not analyze for C or N.

PHYSICAL AND OPTICAL PROPERTIES

Crystals of phoxite are composite blades, up to about 0.4 mm in maximum dimension, growing in complex intergrowths (Figs. 1, 2, and 3). The blades are flattened on {100} and elongated and striated along [001]. The crystal forms {100}, {010}, {110}, {011}, {120}, and {11$\overline{1}$} (Fig. 4) were identified based upon careful observations during the single-crystal XRD and optical studies. Reflected-light measurements were not possible because of the complex intergrowths of crystals and the generally poorly formed, stepped nature of crystal faces. No twinning was observed.

The crystals are colorless, but usually appear light to medium brown or beige due to inclusions. The streak is white and the luster is vitreous to oily. Phoxite is non-fluorescent in long- or short-wave ultraviolet light. It has a Mohs hardness of 2½ based upon scratch tests. Crystals are brittle with irregular fracture and exhibit a fair {100} cleavage. The density measured by floatation in a mixture of methylene iodide and toluene is 1.98(2) g/cm³. The calculated density is 1.987 g/cm³ using the empirical formula and 1.965 g/cm³ using the ideal formula. The mineral is insoluble at room temperature in H_2O, strong acids (HCl, H_2SO_4, HNO_3) and strong base (concentrated NaOH aqueous solution).

Phoxite is optically biaxial (–) with α = 1.499(1), β = 1.541(1), γ = 1.542(1) determined in white light. The measured

FIGURE 1. Circular structure comprised largely of phoxite crystals; note colorless/white rim of struvite crystals; field of view 3.4 mm across. (Color online.)
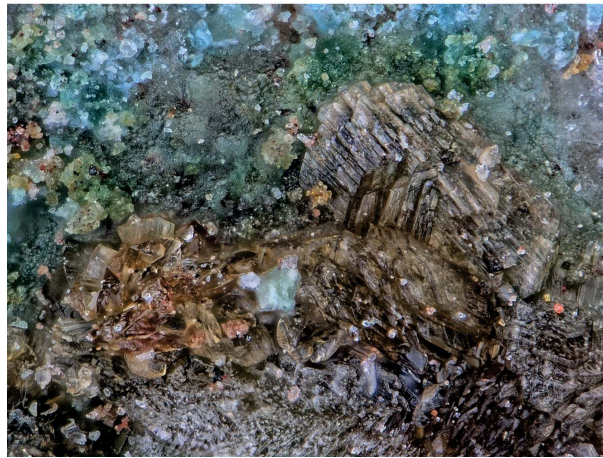

FIGURE 2. Intergrowth of light brown to beige phoxite crystals. Note large composite blade on right side; field of view 0.65 mm across. (Color online.)
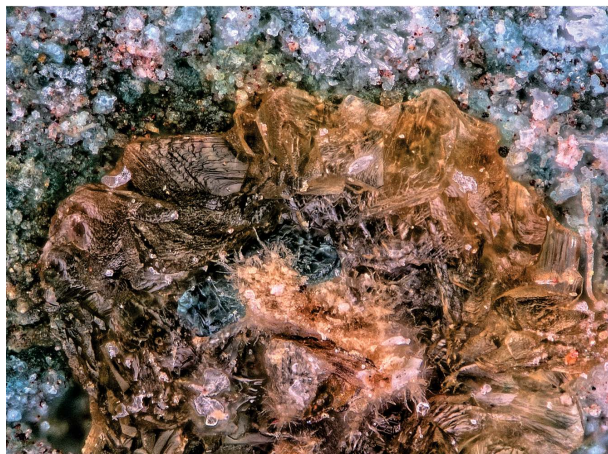
FIGURE 3. Intergrowth of light to dark beige phoxite crystals with blue antipinite crystal near center; field of view 0.68 mm across. (Color online.)
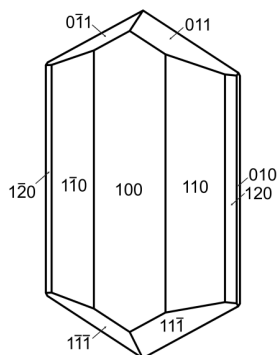

FIGURE 5. Raman spectrum of phoxite. (Color online.)

FIGURE 4. Crystal drawing of phoxite; clinographic projection.

$2V$ is 16(1)° and the calculated $2V$ is 17.2°. Slight $r < v$ dispersion was observed. The optical orientation is $Y = \mathbf{b}$, $X \wedge \mathbf{a} \approx 9°$ in obtuse β. No pleochroism was observed.

Raman spectroscopy

Raman spectroscopy was conducted on a Horiba XploRa+ micro-Raman spectrometer at the Natural History Museum of Los Angeles. Attempts were made to measure the Raman spectrum with a 532 nm laser; however, phoxite was susceptible to burning by the beam due to the ~2 μm spot size even at the lowest power setting (30 μW). Consequently, the spectrum was measured using an incident wavelength of 785 nm, laser slits of 100 μm, 1800 gr/mm diffraction grating and a 100× (0.9 NA) objective. Data were collected for ~12 min at a maximum laser power of 19.0 mW at the sample, which achieved a sufficient signal-to-noise ratio without altering the spectrum during data collection.

The Raman spectrum of phoxite is shown in Figure 5 and bands are listed in Table 1. Phoxite has several characteristic regions for phosphate, oxalate, and ammonium and these modes can be matched and visualized from Wurm database (http://www.wurm.info/; Caracas and Bobocioiu 2011) of computed
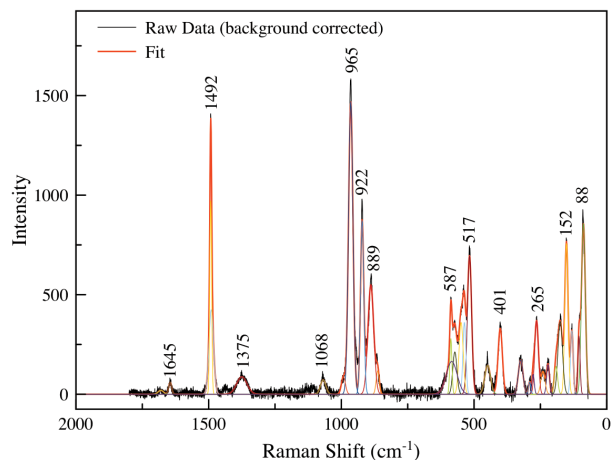
properties for minerals. The Raman bands centered between 965 and 889 cm^{-1} were assigned to P-O stretches of the phosphate group, 1068 and 992 cm^{-1} were assigned to the P-O stretches associated with protonated phosphate, 1492 through 1375 cm^{-1} were assigned to C-C and C-O stretches of oxalate (e.g., as seen in caoxite). There is an indication that the NH$_4$ bending mode appears in Raman spectrum at 1645 cm^{-1}, similar to struvite (http://rruff.info/; Lafuente et al. 2015), the symmetric stretching in teschemacherite and twisting in barberiite.

TABLE 1. Raman bands and their vibrational mode assignments for phoxite

Band no.	Intensity (%)	Position (cm^{-1})	HWHM (cm^{-1})	Vibrational mode assignments[a]
1	2	1680	12	NH$_4$ bending
2	3	1645	7	NH$_4$ bending
3	27	1492	4	possible NH$_4$ bending, OH bending, C-O + C-C sym. stretching
4	30	1490	10	C-O sym. stretching; O-C-O bending
5	14	1375	23	COO rocking, NH$_4$ bending
6	6	1069	12	P-O asym. stretching in HPO$_4$
7	5	992	9	P-O stretching in HPO$_4$
8	100	965	10	P-O stretching
9	44	922	7	C-C stretching
10	49	889	13	
11	6	863	7	
12	27	584	24	ν$_4$ PO$_4$ bending
13	9	587	5	
14	13	572	9	
15	23	549	9	
16	16	536	7	unassigned
17	45	517	9	ν$_2$ PO$_4$ bending
18	13	449	13	ν$_2$ PO$_4$ bending
19	22	401	10	Mg-O stretching
20	12	324	10	
21	2	290	5	
22	4	277	5	
23	20	264	8	
24	7	240	9	lattice modes
25	6	221	6	
26	7	191	7	
27	26	175	10	
28	37	152	7	
29	13	131	6	
30	10	105	5	
31	51	88	9	

[a] Raman modes determined by comparative analysis of DFT calculations from the http://wurm.info/ database.

Chemical analysis

Analyses of phoxite (7 points over 4 crystals) were performed at the University of Utah on a Cameca SX-50 electron microprobe with four wavelength-dispersive spectrometers utilizing Probe for EPMA software. Analytical conditions were 15 keV accelerating voltage, 5 nA beam current, and a beam diameter of 10 μm. Counting times were 30 s on peak and 15 s on background for each element. Raw X-ray intensities were corrected for matrix effects with a φρ(z) algorithm (Pouchou and Pichoir 1991). Severe damage from the electron beam was observed. Attempts to analyze N (syn. Cr_2N standard) provided a wide range of values [$(NH_4)_2O$: 5.26–10.53 wt%]. This is assumed to be due to variable loss of NH_4 under the beam. The highest value obtained for $(NH_4)_2O$ closely corresponds to the ideal amount of NH_4 when combined with analyzed K, which would share the same structural site.

CHN analysis conducted at the Marine Sciences Institute, University of California at Santa Barbara provided C 6.95, H 3.91, and N 4.32 wt%, which corresponds to C_2O_3 20.83, H_2O 23.78, and $(NH_4)_2O$ 8.04 wt%. Because of the small sample mass (1.2 mg), the presence of inclusions of other unidentified phases in phoxite crystals and the unavoidable incorporation of associated phases in the analyzed sample, these values are considered to be rough approximations, at best. Consequently, $(NH_4)_2O$, C_2O_3, and H_2O calculated from the structure determination are used for the empirical formula. The loss of NH_4 and H_2O during and/or prior to (due to vacuum) the analyses results in significantly higher concentrations for the remaining constituents than are to be expected; therefore, the other analyzed constituents have then been normalized to provide a total of 100%. Analytical data are given in Table 2.

The empirical formula (based on 2 P and 16 O apfu) is $[(NH_4)_{1.77}K_{0.23}]_{\Sigma2}Mg_{2.00}(C_2O_4)(PO_3OH)_2(H_2O)_4$. The simplified formula is $(NH_4)_2Mg_2(C_2O_4)(PO_3OH)_2(H_2O)_4$, which requires $(NH_4)_2O$ 11.92, MgO 18.46, P_2O_5 32.50, C_2O_3 16.49, H_2O 20.63, total 100 wt%. The Gladstone-Dale compatibility (Mandarino 2007) $1 - (K_p/K_c)$ is –0.007 in the range of superior compatibility.

X-ray crystallography and structure determination

Powder X-ray studies were carried out using a Rigaku R-Axis Rapid II curved imaging plate microdiffractometer with monochromatized MoKα radiation. A Gandolfi-like motion on the φ and ω axes was used to randomize the sample. Observed d-values and intensities were derived by profile fitting using JADE 2010 software (Materials Data, Inc.). The powder data are presented in Supplemental[1] Table S1. Unit-cell parameters refined from the powder data using JADE 2010 with whole pattern fitting are $a = 7.294(4)$ Å, $b = 13.565(4)$ Å, $c = 7.834(4)$ Å, $β = 108.317(15)°$, and $V = 735.8(6)$ Å^3.

Single-crystal X-ray studies were carried out using the same diffractometer and radiation used for the powder study. The Rigaku CrystalClear software package was used for processing the structure data, including the application of an empirical multiscan absorption correction using ABSCOR (Higashi 2001). The structure was solved by direct methods using SIR2011 (Burla et al. 2012) and SHELXL-2016 (Sheldrick 2015) was used for the refinement of the structure. All non-hydrogen sites were refined with anisotropic displacement parameters. All H atoms were located in difference Fourier maps and these sites were successfully refined with isotropic displacement parameters without distance or displacement parameter restraints. The N site was refined with joint occupancy by N and K, with the occupancies of the H sites associated with N tied to the N occupancy. This yielded $(NH_4)_{0.923}K_{0.077}$, compared to $(NH_4)_{0.885}K_{0.115}$ provided by the EPMA. Data collection and refinement details are given in Table 3, atom coordinates and displacement parameters in Supplemental[1] Table S2, selected bond distances in Supplemental[1] Table S3, and a bond-valence analysis in Table 4.

DESCRIPTION OF THE STRUCTURE

The structure of phoxite contains NH_4 (ammonium), PO_3OH (hydrogen phosphate) and C_2O_4 (oxalate) groups, and $MgO_4(H_2O)_2$ octahedra. The C_2O_4 group forms bidentate linkages with two equivalent Mg-centered octahedra, that is, by sharing two cis O atoms with each octahedron. The pair of $MgO_4(H_2O)_2$ octahedra linked by the central oxalate group forms a $Mg_2(C_2O_4)O_4(H_2O)_4$ unit. Of the four vertices of each octahedron that do not participate in the bidentate oxalate linkage, two cis vertices are O atoms of H_2O groups and two cis vertices are shared with PO_3OH tetrahedra. The PO_3OH tetrahedra each share two non-OH vertices with Mg-centered octahedra in different $Mg_2(C_2O_4)O_4(H_2O)_4$ units. The linkages between the PO_3OH tetrahedra and the $Mg_2(C_2O_4)O_4(H_2O)_4$ units result in an undulating

TABLE 2. Chemical compositions (wt%) of phoxite

Constituent	Mean	Min.	Max.	S.D.	Standard	Normalized
$(NH_4)_2O$*						10.44
K_2O	2.74	2.07	3.36	0.45	sanidine	2.45
MgO	20.43	20.08	20.86	0.27	diopside	18.25
P_2O_5	35.98	35.39	36.67	0.51	apatite	32.15
C_2O_3*						16.31
H_2O*						20.40
Total						100.00
* Based on the structure.						

TABLE 3. Data collection and structure refinement details for phoxite

Diffractometer	Rigaku R-Axis Rapid II
X-ray radiation/power	MoKα (λ = 0.71075 Å)/50 kV, 40 mA
Temperature	293(2) K
Structural formula	$[(NH_4)_{0.923}K_{0.077}]_2Mg_2(C_2O_4)(PO_3OH)_2(H_2O)_4$
Space group	$P2_1/c$
Unit-cell dimensions	$a = 7.2962(3)$ Å
	$b = 13.5993(4)$ Å
	$c = 7.8334(6)$ Å
	$β = 108.271(8)°$
V	738.07(7) Å^3
Z	2
Density (for above formula)	1.980 g/cm^3
Absorption coefficient	0.52 mm^{-1}
F(000)	454
Crystal size	100 × 60 × 40 μm
θ range	3.00 to 24.98°
Index ranges	$-8 ≤ h ≤ 8, -16 ≤ k ≤ 16, -9 ≤ l ≤ 9$
Refls collected/unique	8153/1305; $R_{int} = 0.034$
Reflections with $I_o > 2σI$	665
Completeness to θ = 24.98°	99.8%
Refinement method	Full-matrix least-squares on F^2
Parameters/restraints	145/0
GoF	1.108
Final R indices (I > 2σI)	$R_1 = 0.0275, wR_2 = 0.0693$
R indices (all data)	$R_1 = 0.0327, wR_2 = 0.0722$
Largest diff. peak/hole	$+0.29/-0.33$ e·A^{-3}

Notes: $R_{int} = Σ|F_o^2 - F_o^2(mean)|/Σ[F_o^2]$. GoF = $S = \{Σ[w(F_o^2 - F_c^2)^2]/(n - p)\}^{1/2}$. $R_1 = Σ||F_o| - |F_c||/Σ|F_o|$. $wR_2 = \{Σ[w(F_o^2 - F_c^2)^2]/Σ[w(F_o^2)^2]\}^{1/2}$; $w = 1/[σ^2(F_o^2) + (aP)^2 + bP]$, where a is 0.0388, b is 0.323, and P is $[2F_c^2 + Max(F_o^2,0)]/3$.

TABLE 4. Bond-valence analysis for phoxite[a]

	NH₄	Mg	P	C	Hydrogen bonds		Σ
					Accepted	Donated	
O1	0.13, 0.11	0.32		1.43			1.99
O2	0.07	0.30		1.43	0.19		1.99
O3	0.19	0.39	1.32				1.90
O4	0.09	0.40	1.27		0.22		1.98
O5	0.19		1.26		0.28, 0.20		1.93
OH			1.08		0.12	−0.28	0.92
OW1	0.08, 0.06	0.36				−0.20, −0.19	0.11
OW2	0.10	0.29			−	−0.22, −0.12	0.05
C				0.98			
Σ	1.02	2.06	4.93	3.84			

Note: Values are expressed in valence unit.
[a] NH₄–O bond-valence parameters are from Garcia-Rodriguez et al. (2000). Mg^{2+}–O, P^{5+}–O, and C^{4+}–O bond-valence parameters are from Gagné and Hawthorne (2015). C-C bond-valence parameters are from D.l. Brown (pers. comm.). Hydrogen-bond strengths are based on O-O bond lengths from Ferraris and Ivaldi (1988).

$[Mg_2(C_2O_4)(PO_3OH)_2(H_2O)_4]^{2-}$ sheet (Fig. 6). The NH_4^+ is located in the interlayer (Fig. 7) and forms bonds to O atoms in adjacent sheets. The NH_4-O bonding is described below.

Hydrogen bonding

Hydrogen bonding between the OH and H_2O hydrogen atoms and other O atoms serve as additional linkages both within and between the sheets. The OH-HOH···O5 hydrogen bond, between the OH of the PO_3OH group in one sheet and the O5 of the PO_3OH group in an adjacent sheet and with an OH···O5 distance of only 2.611(2) Å, is a particularly strong linkage between the structural sheets. The strength of this bond is comparable to that of some of the Mg-O bonds. The OW1 group forms two relatively strong hydrogen bonds, one intersheet bond (OW1-H1b···O2; 2.278 Å) to a PO_3OH group and one intrasheet bond, (OW1-H1a···O2; 2.749 Å) to a C_2O_4 group. The OW2 group forms two intrasheet hydrogen bonds to O atoms of PO_3OH groups, one of which (OW2-H2b···O4; 2.710 Å) is relatively strong. The network of linkages created by the four strongest hydrogen bonds is shown in Figure 8. Because of the strong hydrogen bonds between the sheets, the phoxite structure can be considered a "soft framework," with channels containing NH_4^+.

NH₄-O bonding

The NH_4-O bond lengths in the structure of phoxite vary from 2.839 to 3.272 Å, corresponding to a coordination of nine. In surveying NH_4-containing structures, Khan and Baur (1972) found NH_4-O coordinations from 4 to 9. They concluded that for small (4 or 5) coordinations, the NH_4 group behaves more like a conventional hydrogen-bond donor, forming nearly linear N-H···O bonds, while for higher coordinations, the NH_4 group behaves more like an alkali cation, with the NH_4 group exhibiting orientational disorder or the H bonds being polyfurcated. In the crystal structure of hannayite, $Mg_3(NH_4)_2(HPO_4)_4·8H_2O$, Catti and Franchini-Angels (1976) described the hybrid (or dual) bonding behavior of the NH_4^+ group. They noted that, for short H···O bonds with large N-H···O angles, the NH_4^+ group behaves as an ordered hydrogen-bond donor, while long H···O distances and relatively small N-H···O angles are indicative of behavior as a strongly electropositive large alkali-like cation. They suggested that this dual behavior for NH_4^+ appears to be

quite common. The dual-bonding behavior of NH_4^+ is clearly observed in the structure of phoxite (Supplemental[1] Table S3; Fig. 9); each of the H atoms associated with the NH_4^+ group forms a single short, nearly linear hydrogen bond to an O atom, while other NH_4-O bonds are more appropriately regarded as electrostatic in nature.

García-Rodríguez et al. (2000) studies bond valences related to NH_4^+ groups, treating NH_4^+ strictly as a spherical cation. Their bond-valence parameters provide reasonable bond-valence sums for phoxite (Table 4). It seems reasonable to assume
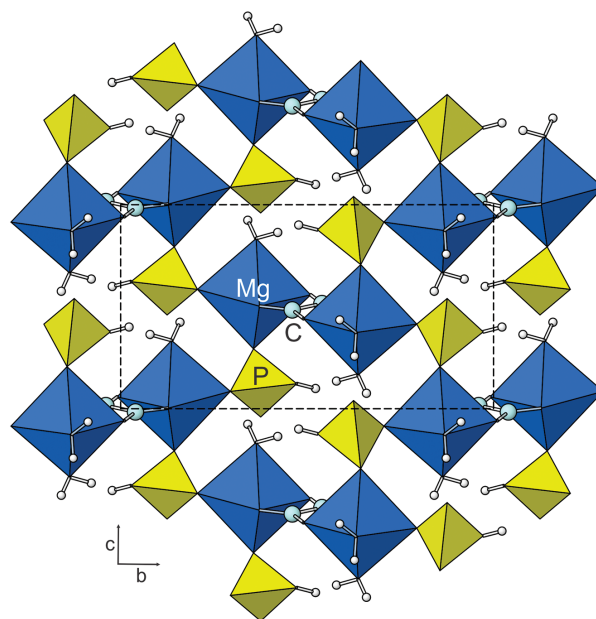

FIGURE 6. $[Mg_2(C_2O_4)(PO_3OH)_2(H_2O)_2]^{2-}$ sheet in the structure of phoxite viewed down [100]. (Color online.)
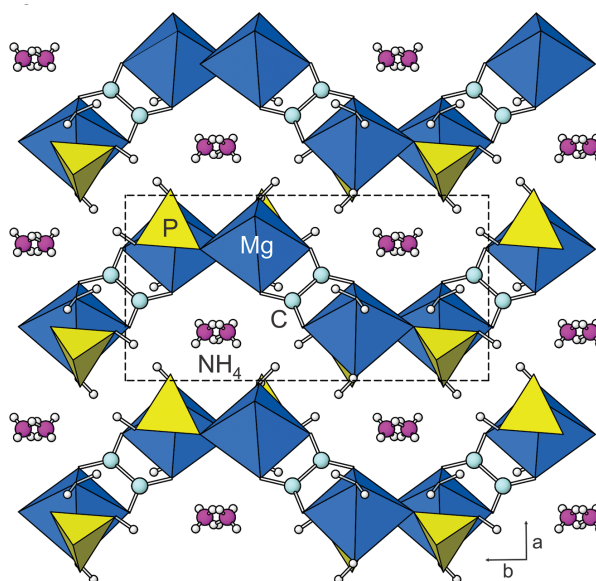

FIGURE 7. Structure of phoxite viewed down [001]. (Color online.)
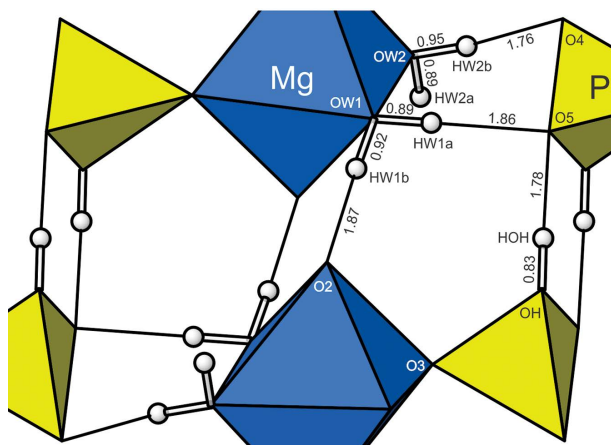
FIGURE 8. Strong hydrogen bonds (shown as single black lines) in the structure of phoxite. Intersheet bonds are approximately vertical (parallel to **b**); intrasheet bonds are approximately horizontal (parallel to **c**). (Color online.)
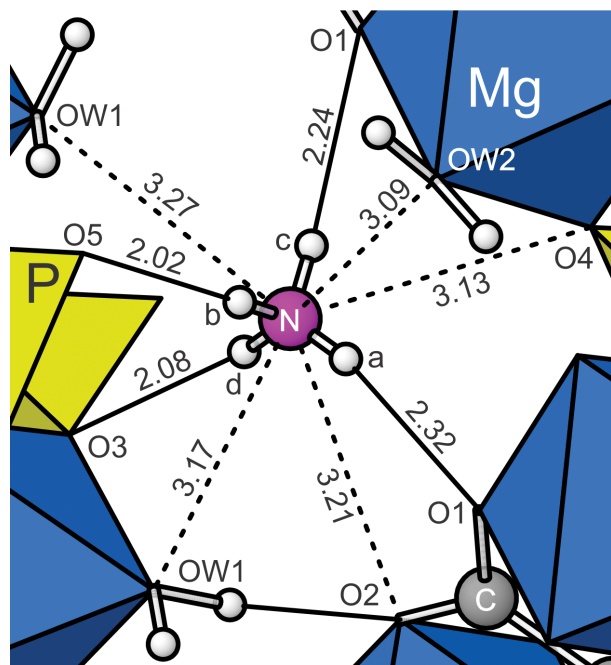

FIGURE 9. The NH_4–O bonding in the structure of phoxite. Ordered hydrogen bonds are shown as solid lines and electrostatic bonds are shown as dashed lines. Note that the N–H distances (not shown) range from 0.74 to 0.84 Å based on the unrestrained structure refinement using XRD data. (Color online.)

that NH_4-O bonds corresponding to the ordered hydrogen bonds that provide somewhat greater bond strength than those corresponding to electrostatic bonds, but for bond-valence calculations, this appears to be adequately accounted for in the García-Rodríguez et al. (2000) approach by the fact that these bonds are generally shorter.

Structural comparisons

Because phoxite is the first mineral known to contain both phosphate and oxalate groups as essential components, it is not surprising that its structure is not closely related to that of any other mineral (cf. Echigo and Kimata 2010; Baran 2014; Piro et al. 2016). The only other oxalate minerals that also include tetrahedral anions are the REE sulfate-oxalates coskrenite-(Ce) (Peacor et al. 1999), levinsonite-(Y), and zugshunstite-(Ce) (Rouse et al. 2001). The overall structural motifs in these sulfate-oxalate minerals are quite different from those in phoxite. While bidentate linkages between oxalate groups and cations are typical in the structures of minerals and synthetic phases, they usually are propagated into infinite structural units, such as the chains in the minerals with the humboltine structure.

We are unaware of any synthetic phase with a structure based on a sheet identical to that in phoxite, but there are structures with locally similar linkages. For example, Huang and Lii (1998) report a framework structure for $[C_4H_{12}N_2][In_2(C_2O_4)(HPO_4)_3]·H_2O$ that is based upon pairs of In-centered octahedra joined by bidentate linkages to a central C_2O_4 group; however, in this phase, all four of the remaining O vertices of each octahedron are shared with a PO_4 group. Another example is the sheet structure of $(NH_4)_2[VO(HPO_4)]_2(C_2O_4)·5H_2O$ reported by Do et al. (2000), in which pairs of highly distorted V-centered octahedra are joined by bidentate linkages to a central C_2O_4 group. In this case, three of the remaining O vertices of each octahedron are shared with a PO_4 group, while the fourth O forms a short vanadyl bond with the V.

IMPLICATIONS

In recent years, there has been a great deal of research on synthetic phosphate-oxalates, particularly focusing on the fabrication of porous framework structures, which take advantage of the ability of the oxalate group to form strong bidentate linkages with octahedrally coordinated cations (cf. Chen et al. 2004). Such frameworks have potential applications in catalysis, adsorption, ion exchange, gas storage, separation, and sensing (cf. Luan et al. 2015). The structure of phoxite is based upon linkages between oxalate groups, phosphate groups, and octahedrally coordinated Mg, which result in a sheet, rather than a three-dimensional framework. Nevertheless, the unique topology of the sheet structural unit in phoxite, the fact that the structure has formed without the need for an organic templating agent, and the occurrence of the phase in nature all have the potential to provide valuable insights into this important class of compounds. Another avenue worth investigating is whether the strong hydrogen bonding between the undulating sheets gives the phoxite structure soft-framework character that may be useful for ion exchange and, perhaps, expansion of the interlayer region between the sheets could allow for the accommodation of larger molecules. Ion exchange properties may be particularly interesting for agriculture applications, including the mitigation of over-fertilization practices and the treatment of saline irrigation water, while the oxalate would provide a natural pesticide defense for crops. A caveat in this regard is that the ordered hydrogen bonding of the NH^{4+} cation to surrounding O atoms is indicative of a well-defined structural role for NH^{4+}, which could inhibit ion exchange.

REFERENCES CITED

Anstoetz, M., Rose, T.J., Clark, M.W., Yee, L.H., Raymond, C.A., and Vancov, T. (2015) Novel applications for oxalate-phosphate-amine metal-organic-frameworks (OPA-MOFs): Can an iron-based OPA-MOF be used as slow-release fertilizer?. PLOS One, 10, e0144169.

Baran, E.J. (2014) Natural oxalates and their analogous synthetic complexes. Journal of Coordination Chemistry, 67, 3734–3768.

Bernardi, A.C.C., Polidoro, J.C., de Melo Monte, M.B., Pereira, E.I., de Oliveira, C.R., and Ramesh, K. (2016) Enhancing nutrient use efficiency using zeolites minerals—A review. Advances in Chemical Engineering and Science, 6, 295.

Bridge, P.J. (1977) Archerite, (K,NH$_4$)H$_2$PO$_4$, a new mineral from Madura, Western Australia. Mineralogical Magazine, 41, 33–35.

Burla, M.C., Caliandro, R., Camalli, M., Carrozzini, B., Cascarano, G.L., Giacovazzo, C., Mallamo, M., Mazzone, A., Polidori, G., and Spagna, R. (2012) SIR2011: a new package for crystal structure determination and refinement. Journal of Applied Crystallography, 45, 357–361.

Catti, M., and Franchini-Angela, M. (1976) Hydrogen bonding in the crystalline state. Structure of Mg$_3$(NH$_4$)$_2$(HPO$_4$)$_4$·8H$_2$O (hannayite), and crystal-chemical relationships with schertelite and struvite. Acta Crystallographica, B32, 2842–2848.

Caracas, R., and Bobocioiu, E. (2011) The WURM project—a freely available web-based repository of computed physical data for minerals. American Mineralogist, 96, 437–443.

Chen, Z., Weng, L., Chen, J., and Zhao, D. (2004) Hydrothermal synthesis and characterization of new hybrid open-framework indium phosphate-oxalates. Chinese Science Bulletin, 49, 658–664.

Chukanov, N.V., Aksenov, S.M., Rastsvetaeva, R.K., Lyssenko, K.A., Belakovskiy, D.I., Färber, G., Möhn, G., and Van, K.V. (2015) Antipinite, KNa$_3$Cu$_2$(C$_2$O$_4$)$_4$, a new mineral species from a guano deposit at Pabellón de Pica, Chile. Mineralogical Magazine, 79, 1111–1121.

Do, J., Bontchev, R.P., and Jacobson, A.J. (2000) A hydrothermal investigation of the ½V$_2$O$_5$−H$_2$C$_2$O$_4$/H$_3$PO$_4$/NH$_4$OH system: synthesis and structures of (NH$_4$)VOPO$_4$·1.5H$_2$O, (NH$_4$)$_{0.5}$VOPO$_4$·1.5H$_2$O, (NH$_4$)$_2$[VO(H$_2$O)$_3$]$_2$[VO(H$_2$O)][VO(PO$_4$)$_2$]$_2$·3H$_2$O, and (NH$_4$)$_2$[VO(HPO$_4$)]$_2$(C$_2$O$_4$)·5H$_2$O. Inorganic Chemistry, 39, 3230–3237.

Echigo, T., and Kimata, M. (2010) Crystal chemistry and genesis of organic minerals: a review of oxalate and polycyclic aromatic hydrocarbon minerals. Canadian Mineralogist, 48, 1329–1357.

Eroglu, N., Emekci, M., and Athanassiou, C.G. (2017) Applications of natural zeolites on agriculture and food production. Journal of the Science of Food and Agriculture, 97, 3487–3499.

Ferraris, G., and Ivaldi, G. (1988) Bond valence vs. bond length in O···O hydrogen bonds. Acta Crystallographica, B44, 341–344.

Gagné, O.C., and Hawthorne, F.C. (2015) Comprehensive derivation of bond-valence parameters for ion pairs involving oxygen. Acta Crystallographica, B71, 562–578.

García-Rodríguez, L., Rute-Pérez, Á., Piñero, J.R., and González-Silgo, C. (2000) Bond-valence parameters for ammonium-anion interactions. Acta Crystallographica, B56, 565–569.

Higashi, T. (2001) ABSCOR. Rigaku Corporation, Tokyo.

Huang, Y.F., and Lii, K.H. (1998) Organically templated inorganic/organic hybrid materials: hydrothermal synthesis and structural characterization of [C$_4$H$_{12}$N$_2$][In$_2$(C$_2$O$_4$)(HPO$_4$)$_3$]·H$_2$O. Journal of the Chemical Society, Dalton Transactions, 24, 4085–4086.

Kampf, A.R., Cooper, M.A., Nash, B.P., Cerling, T., Marty, J., Hummer, D.R., Celestian, A.J., Rose, T.P., and Trebisky, T.J. (2017) Rowleyite, [Na(NH$_4$,K)$_9$Cl$_4$][V$_2^{5+,4+}$(P,As)O$_8$]$_6$·n[H$_2$O,Na,NH$_4$,K,Cl], a new mineral with a mesoporous framework structure. American Mineralogist, 102, 1037–1044.

Khan, A.A., and Baur, W.H. (1972) Salt hydrates. VIII. The crystal structures of sodium ammonium orthochromate dihydrate and magnesium diammonium bis(hydrogen orthophosphate) tetrahydrate and a discussion of the ammonium ion. Acta Crystallographica, B28, 683–693.

Lafuente, B., Downs R.T., Yang. H., and Stone, N. (2015) The power of databases: the RRUFF project. In T. Armbruster and R.M. Danisi, Eds., Highlights in Mineralogical Crystallography, p. 1–30. De Gruyter.

Luan, L., Li, J., Chen, C., Lin, Z., and Huang, H. (2015) Solvent-free synthesis of crystalline metal phosphate oxalates with a (4,6)-connected fsh topology. Inorganic Chemistry, 54, 9387–9389.

Mandarino, J.A. (2007) The Gladstone–Dale compatibility of minerals and its use in selecting mineral species for further study. Canadian Mineralogist, 45, 1307–1324.

Nakata, P.A. (2003) Advances in our understanding of calcium oxalate crystal formation and function in plants. Plant Science, 164, 901–909.

——— (2015) An assessment of engineered calcium oxalate crystal formation on plant growth and development as a step toward evaluating its use to enhance plant defense. PLOS One, 10, e0141982.

Peacor, D.R., Rouse, R.C., and Essene, E.J. (1999) Coskrenite-(Ce), (Ce,Nd,La)$_2$(SO$_4$)$_2$(C$_2$O$_4$)·8H$_2$O, a new rare-earth oxalate mineral from Alum Cave Bluff, Tennessee: characterization and crystal structure. Canadian Mineralogist, 37, 1453–1462.

Piro, O.E., Echeverría, G.A., González-Baró, A.C., and Baran, E.J. (2016) Crystal and molecular structure and spectroscopic behavior of isotypic synthetic analogs of the oxalate minerals stepanovite and zhemchuzhnikovite. Physics and Chemistry of Minerals, 43, 287–300.

Pouchou, J.-L., and Pichoir, F. (1991) Quantitative analysis of homogeneous or stratified microvolumes applying the model "PAP." In K.F.J. Heinrich and D.E. Newbury, Eds., Electron Probe Quantitation, pp. 3l–75. Plenum Press, New York.

Reháková, M., Čuvanová, S., Dzivak, M., Rimár, J., and Gaval'Ova, Z. (2004) Agricultural and agrochemical uses of natural zeolite of the clinoptilolite type. Current Opinion in Solid State and Materials Science, 8, 397–404.

Rouse, R.C., Peacor, D.R., Essene, E.J., Coskren, T.D., and Lauf, R.J. (2001) The new minerals levinsonite-(Y) [(Y, Nd,Ce)Al(SO$_4$)$_2$(C$_2$O$_4$)·12H$_2$O] and zugshunstite-(Ce) [(Ce,Nd,La)Al(SO$_4$)$_2$(C$_2$O$_4$)·12H$_2$O]: Coexisting oxalates with different structures and differentiation of LREE and HREE, Geochimica et Cosmochimica Acta, 65, 1101–1115.

Sheldrick, G.M. (2015) Crystal Structure refinement with SHELX. Acta Crystallographica, C71, 3–8.

Usman, K.A.S., Buenviaje, S.C. Jr., Edañol, Y.D.G., Conato, M.T., and Payawan, L.M. Jr. (2018) Facile fabrication of a potential slow-release fertilizer based on oxalate-phosphate-amine metal-organic frameworks (OPA-MOFs). Materials Science Forum, vol. 936, pp. 14–19. Trans Tech Publications.

Wilson, W.E., and Miller, D.K. (1974) Minerals of the Rowley mine. Mineralogical Record, 5, 10–30.

Endnote:

[1] Deposit item AM-19-76991, CIF and Supplemental Tables. Deposit items are free to all readers and found on the MSA website, via the specific issue's Table of Contents (go to http://www.minsocam.org/MSA/AmMin/TOC/2019/Jul2019_data/Jul2019_data.html).